Electronic Supplementary Information (ESI)

Pyridoxal hydrazonato molybdenum(VI) complexes: Assembly, Structure and Epoxidation (Pre)Catalyst testing under solvent-free conditions

Jana Pisk, Biserka Prugovečki, Dubravka Matković-Čalogović, Tomislav Jednačak, Predrag Novak, Dominique Agustin* and Višnja Vrdoljak*

Contents

Ligand preparation

All the ligands were prepared by condensation reaction of the pyridoxal and appropriate hydrazide (isonicotinic acid hydrazide, benzhydrazide, 4–hydroxy benzhydrazide) in methanol. After refluxing the reaction mixture for 3 hours orange (in the case of $\mathbf{H_2L^1}$) and yellow (in the case of $\mathbf{H_2L^2}$ and $\mathbf{H_2L^3}$) precipitates were formed, filtrated and washed with methanol.

$\mathbf{H_2L^1}$ Found: C, 58.63; H, 4.63; N, 19.36; O, 16.61. $C_{14}H_{14}N_4O_3$ requires C, 58.73; H, 4.93; N, 19.57; O, 16.77%. M_p = 230˚C.
$\mathbf{H_2L^2}$ Found: C, 62.97; H, 5.11; N, 14.27; O, 16.63. $C_{15}H_{15}N_3O_3$ requires C, 63.15; H, 5.30; N, 14.73; O, 16.82%. M_p = 220 ˚C.
$\mathbf{H_2L^3}$ Found: C, 59.59; H, 4.91; N, 13.73; O, 21.18. $C_{15}H_{15}N_3O_4$ requires C, 59.79; H, 5.02; N, 13.95; O, 21.24%. M_p = 290 ˚C.

IR comparison

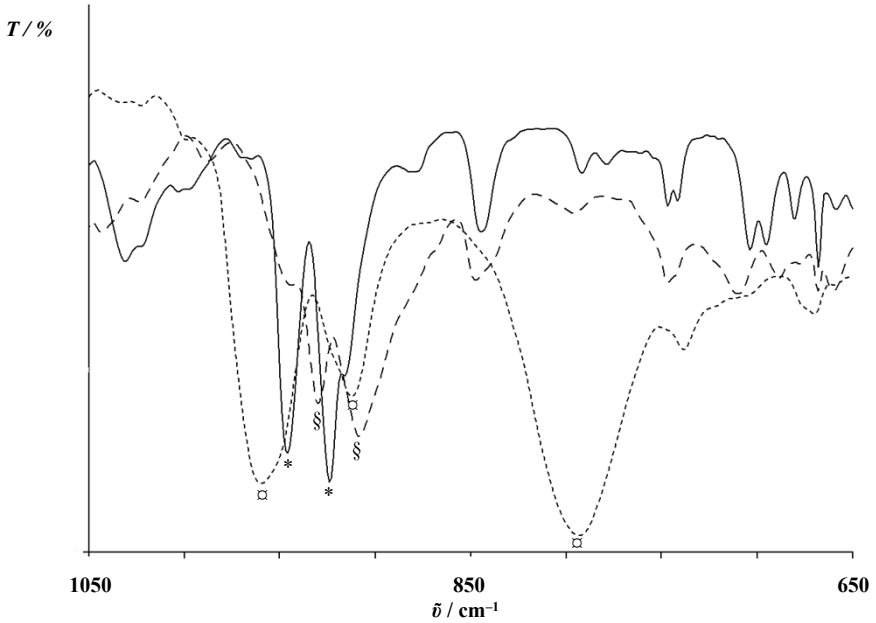

Fig. S1. Comparison of IR spectra of the complex **I** (dashed line), **Ia** (solid line) and **1** (dotted line). Characteristic bands are assigned (§ for the complex **I**, * for the complex **Ia**, ¤ for the complex **1**).

Solid-state transformations – Powder X-ray diffraction patterns

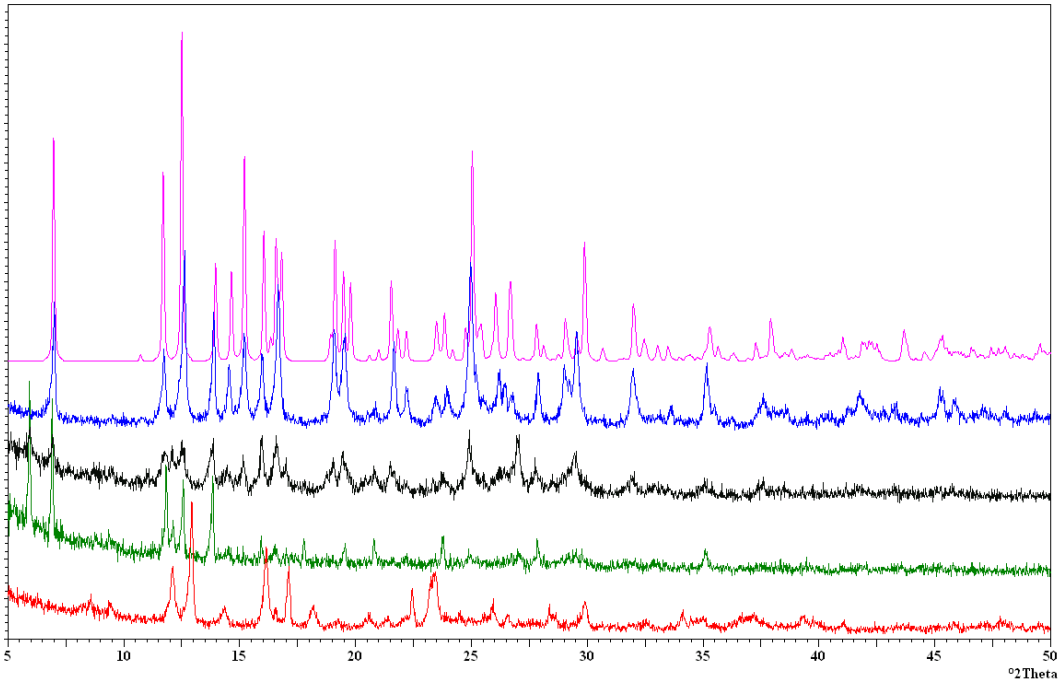

Fig. S2. PXRD patterns: calculated from the crystal structure of the mononuclear complex **Ia** (pink line), of the synthesized mononuclear complex **Ia** (blue line), of the synthesized mononuclear complex **Ia** after 5 min grinding (black line), after heating of the mononuclear complex **Ia** at 200 °C for 3 hours (green line), of the polynuclear complex **I** (red line).

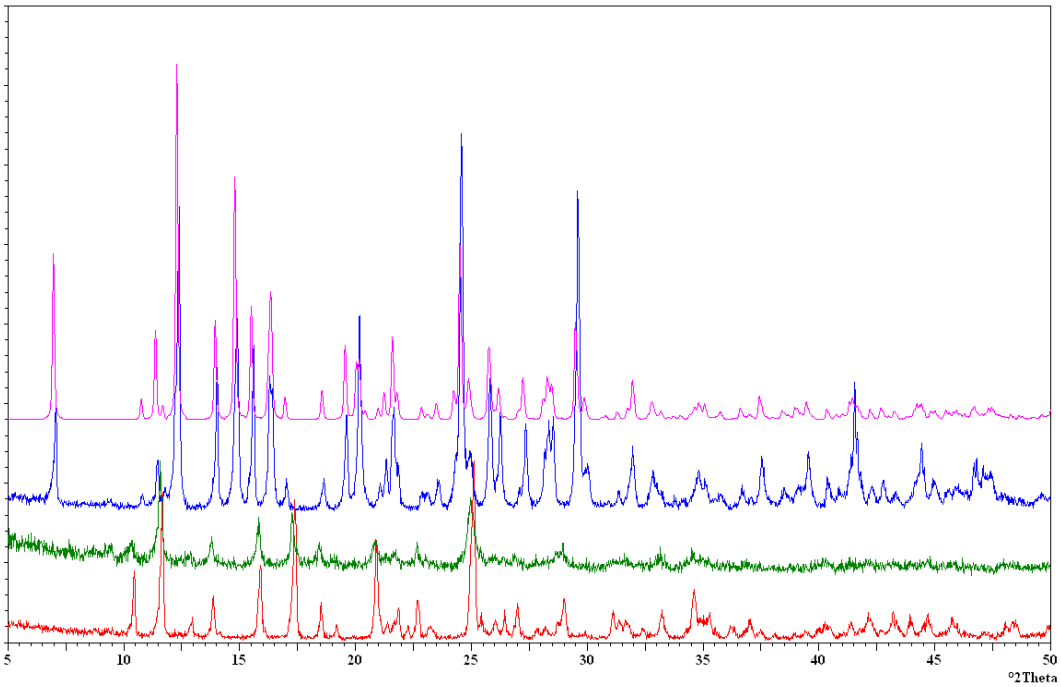

Fig. S3. PXRD patterns: calculated from the crystal structure of the mononuclear complex **IIa** (pink line), of the synthesised mononuclear complex **IIa** (blue line), after heating of the mononuclear complex **IIa** at 200 °C for 3 hours (green line), of the polynuclear complex **II** (red line).

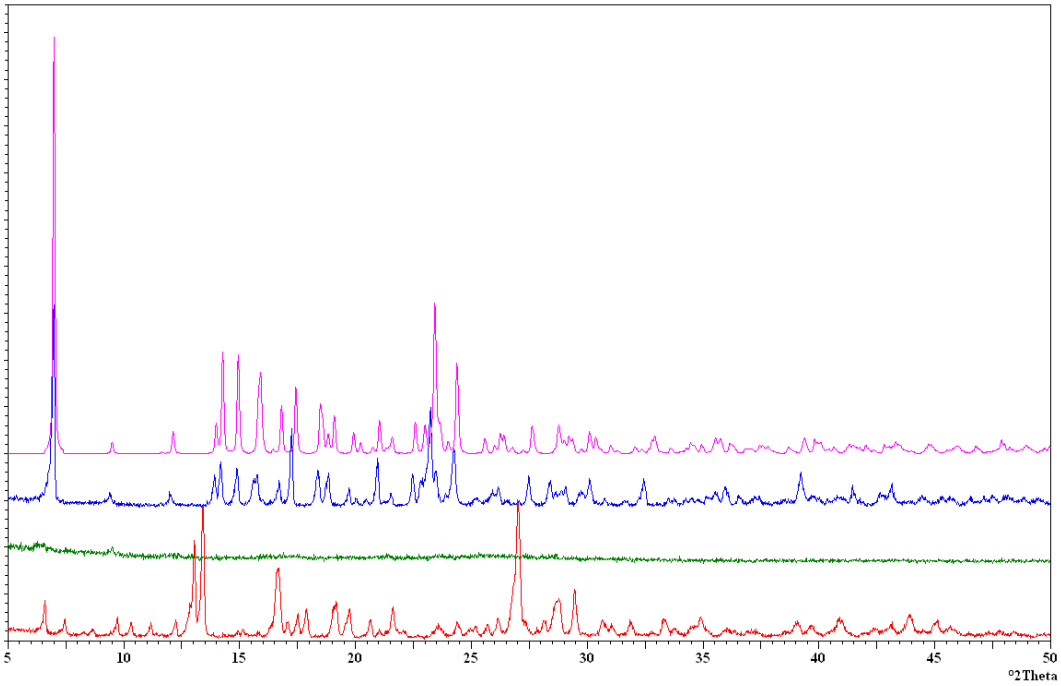

Fig. S4. PXRD patterns: calculated from the crystal structure of the mononuclear complex **IIIa** (pink line), of the synthesised mononuclear complex **IIIa** (blue line), after heating of the mononuclear complex **IIIa** at 120 °C for 3 hours (green line), of the polynuclear complex **II** (red line).

NMR studies

Table S1. ^{1}H and ^{13}C chemical shifts of ligands **H_2L^1**, **H_2L^2**and **H_2L^3** and their molybdenum complexes.

Comp	**H_2L^1**		**Ia**		**H_2L^2**		**IIa**		**H_2L^3**		**IIIa**	
Atom	δ(^{1}H)/ ppm	δ(^{13}C)/ ppm	δ(^{1}H)/ ppm	δ(^{13}C)/ ppm	δ(^{1}H)/ ppm	δ(^{13}C)/ ppm	δ(^{1}H)/ ppm	δ(^{13}C)/ ppm	δ(^{1}H)/ ppm	δ(^{13}C)/ ppm	δ(^{1}H)/ ppm	δ(^{13}C)/ ppm
1	8.20, 1H, s	131.0	8.10, 1H, s	140.7	7.95 1H, s	138.6	8.06 1H, s	140.5	7.95, 1H, s	138.5	8.05, 1H, s	140.5
2												
3	12.89, 1H, br				12.29, 1H, br				12.37, 1H, br			
4		161.8		168.4		162.9		170,0		162.5		170.2
5		139.1		137.1		132.0		129.6		122.5		120.0
6, 10	7.99, 2H, d, ^{3}J = 5.1 Hz	121.8	7.92; 7.93, 2H, d, ^{3}J = 5.2 Hz	121. 7	7.99, 2H, d, ^{3}J = 7.6 Hz	127.7	8.04 2H, d, ^{3}J = 7.7 Hz	128.2	7.90 2H, d, ^{3}J = 8,6 Hz	129.9	7,89 2H, d, ^{3}J = 8,5 Hz	130.5
7, 9	8.86; 8.87, 2H, d, ^{3}J = 5.2 Hz	150.1	8.78; 8.79 2H, d, ^{3}J = 5.3 Hz	150.6	7.55, 2H, dd, $^{3}J_1$ = 7.7 Hz, $^{3}J_2$ = 7.4 Hz	128.6	7.54, 2H, dd, $^{3}J_1$ = 7.9 Hz, $^{3}J_1$ = 7.3 Hz	128.8	6.93 2H, d, ^{3}J = 8,7 Hz	115.2	6.87 2H, d, ^{3}J = 8,4 Hz	115.7
8					7.63, 1H, t, ^{3}J = 7.4 Hz	132.30	7.62, 1H, t, ^{3}J = 7.3 Hz	132.3		161.3		161.5
11		136.3		134.8		132.25		134.5		132.1		134.3
12		125.8		122.4		120.2		122.5		120.4		122.8
13	9.19, 1H, s	145.5	9.19, 1H, s	154.2	8.97, 1H, s	146.4	9.12	152.2	8.94, 1H, s	145.3	9.03, 1H, s	150.5
14												
15		144.2		148.8		147.5		148.6		147.4		148.5
16		152.6		152.4		150.7		152.2		150.6		152.2
17	13.40, 1H, br				12.55, 1H, br				12.37, 1H, br			
18	4.77, 2H, s	58.3	4.76, 2H, s	58.7	4.62, 2H, s	58.9	4.75, 2H, s	58.7	4.63, 2H, s	58.9	4.73, 2H, s	58.8
19	–		5.59, 1H, br		5.39, 1H, br		5.56, 1H, br		5.39, 1H, br		5.54, 1H, br	
20	2.61, 3H, s	15.4	2.41, 3H, s	19.5	2.43, 3H, s	18.8	2.40, 3H, s	19.5	2.44, 3H, s	18.8	2.39, 3H, s	19.6
21									10.28, 1H, br		10.29, 1H, br	

Scheme S1. NMR numbering scheme

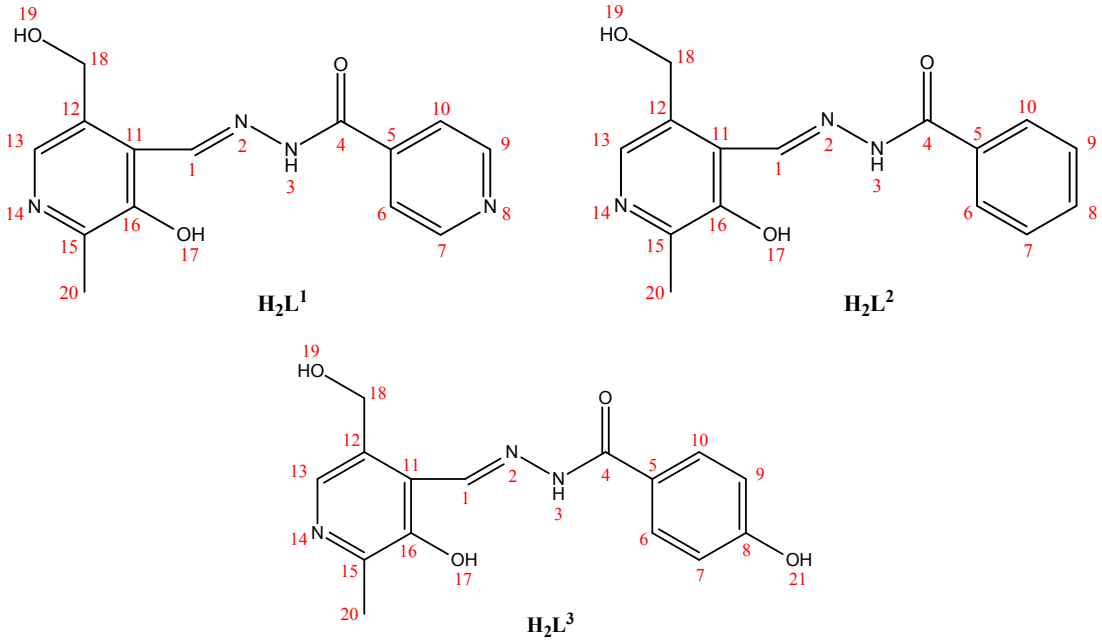

NMR measurements

Proton spectra with spectral width of 6200 Hz and a digital resolution of 0.09 Hz per point were measured with 8 – 16 scans. APT spectra with spectral widths of 7000 Hz and a digital resolution of 0.11 and 0.17 Hz per point, respectively, were collected with 1500 − 12000 scans. Assignment of the ^{1}H and ^{13}C NMR signals was performed using gradient–selected two–dimensional homo– and heteronuclear correlation experiments (gCOSY, gHSQC and gHMBC). In the gCOSY experiment 2046 points in the *f*2 dimension and 512 increments in the *f*1 dimension were used. For each increment 8 scans and the spectral width of 4007 Hz were applied. Digital resolution was 1.97 and 7.82 Hz per point in *f*2 and *f*1 dimensions, respectively. Typical spectral conditions for gHSQC and gHMBC spectra were as follows. Spectral width was 3906 Hz in *f*2 and 18870 Hz in *f*1 dimension for both experiments. 2K data points were applied in the time domains and for each data set 157 and 246 increments were collected for gHSQC and gHMBC spectra, respectively. The resulting digital resolution was 3.81 Hz per point in *f*2 dimension and 34.3 and 36.9 Hz per point in *f*1 dimension in gHSQC and gHMBC spectra, respectively.

UV-Vis spectroscopic studies

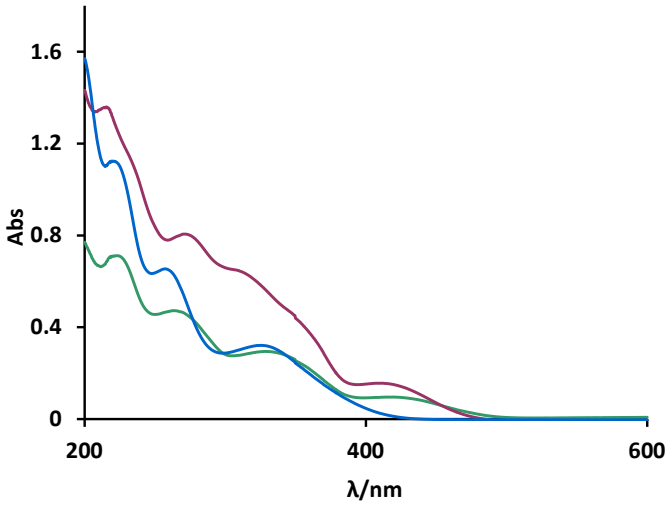

Fig. S5. UV-Vis absorption spectra of $(Bu_4N)_2Mo_6O_{19}$ (blue line), the complex **1** (green line), the complex **Ia** (red line) and absorption maxima. All spectra were recorded in acetonitrile, $c = 5\times10^{-5}$ mol dm^{-3}.

Crystallographic studies

Table S2. Selected bond lengths (Å) and angles (°) for compounds $\mathbf{H_2L^2}$ and **4**.

	$\mathbf{H_2L^2}$	**4**
C1–O1	1.231(2)	1.207(9)
C1–N1	1.353(2)	1.364(9)
C1–C10	1.489(2)	1.500(10)
N1–N2	1.374(2)	1.363(8)
N1–C1	1.352(2)	1.364(9)
N2–C2	1.278(2)	1.288(9)
O1–C1–C10	122.47(16)	120.4(7)
O1–C1–N1	120.98(16)	125.2(7)
N1–C1–C10	116.55(16)	114.4(6)
N2–N1–C1	118.68(14)	118.6(6)
C5–N3–C6	117.84(18)	124.7(6)
C12–N4–C14	–	123.2(8)

Table S3. Geometry of intra- and intermolecular hydrogen bonds (Å, °) for **H_2L^2** , **2**, **4**, **Ia**, **IIa** and **IIIa**.

	D–H···A	D–H (Å)	H···A (Å)	D···A (Å)	D–H···A(°)
H_2L^2	N1–H1···O3[i]	0.86	2.07	2.892(2)	159
	O2–H2···N2	0.82	1.87	2.583(2)	145
	O3–H3···O1[ii]	0.84(2)	1.86(2)	2.701(2)	176(2)
2	N3–H3···O5[iii]	0.88	1.89	2.772(5)	176
	O3–H31···O13[iv]	0.94	1.93	2.731(5)	142
4	N1–H1···O50	0.86	1.88	2.72(3)	165
	O2–H2A···N2	0.82	1.87	2.590(8)	145
	N3– H3···O40[v]	0.86	1.88	2.733(8)	173
	N4–H4A···O30[vi]	0.86	1.87	2.721(9)	171
	O3–H3A···O40	0.82	2.00	2.810(11)	169
Ia	O3A– H3A···N4[vii]	0.82	2.08	2.842(5)	154
	O6–H6···N3[viii]	0.837(19)	1.889(19)	2.722(3)	174(3)
IIa	O3–H3···O6[ix]	0.82	2.09	2.909(3)	177
	O6–H6···N3[x]	0.834(16)	1.891(17)	2.716(2)	170(2)
IIIa	O3–H3···O7[xi]	0.826(17)	2.206(18)	2.986(2)	157.6(19)
	O6–H6···N1[xii]	0.77(2)	1.95(2)	2.7192(19)	177(3)
	O7–H7···O8[xiii]	0.73(3)	1.92(3)	2.648(2)	178(3)
	O8–H8···N3 [xiv]	0.824(14)	1.918(15)	2.730(2)	168.2(18)

[i]1-x,1-y,-z; [ii]x,3/2-y,1/2+z; [iii]1-x,-x+y,2/3-z; [iv]1-y,1+x-y,-1/3+z; [v] -1/2+x,1-y,-1/2+z; [vi]1/2+x,-y,1/2+z; [vii]2-x,1-y,-z; [viii]x,1+y,z; [ix]1-x,1-y,1-z; [x]x,-1+y,z; [xi]x,y,-1+z; [xii]1-x,-y,-z; [xiii]x,y,1+z

Table S4. Selected bond lengths (Å) and angles (°) for compounds **Ia**, **IIa**, **IIIa** and **2**.

	Ia	**IIa**	**IIIa**	**2**
Mo–O1	2.010(2)	1.9899(16)	2.0379(13)	1.981(4)
Mo–O2	1.953(2)	1.9426(16)	1.9325(12)	1.933(3)
Mo–O4	1.700(2)	1.687(2)	1.6987(14)	1.677(3)
Mo–O5	1.699(2)	1.689(2)	1.7015(12)	1.723(3)
Mo–O6	2.327(2)	2.4386(17)	2.2659(14)	–
Mo–N2	2.261(3)	2.260(2)	2.2585(14)	2.231(3)
Mo–O3^{i}	–	–	–	2.380(3)
O1–C1	1.311(3)	1.310(3)	1.309(2)	1.227(8)
N1–N2	1.408(3)	1.387(3)	1.3917(19)	1.390(6)
N1–C1	1.309(3)	1.313(3)	1.309(2)	1.378(8)
N2–C2	1.290(3)	1.284(3)	1.287(2)	1.290(5)
O1–Mo–O2	149.03(9)	147.60(7)	147.16(5)	147.19(13)
O1–Mo–O4	97.16(10)	98.74(8)	95.64(5)	98.41(15)
O1–Mo–O5	98.76(10)	98.43(8)	97.72(5)	94.01(14)
O1–Mo–O6	78.47(9)	77.71(6)	79.32(5)	–
O1–Mo–O3^{i}	–	–	–	78.24(14)
O1–Mo–N2	72.02(9)	71.39(7)	71.26(5)	72.06(12)
O2–Mo–O4	98.66(10)	99.72(8)	99.79(6)	101.43(14)
O2–Mo–O5	102.24(10)	101.61(8)	105.80(5)	104.74(13)
O2–Mo–O6	80.45(9)	79.57(6)	80.92(5)	–
O2–Mo–O3^{i}	–	–	–	77.18(14)
O2–Mo–N2	80.35(9)	80.35(7)	80.12(5)	80.67(12)
O3^{i} –Mo–O4	–	–	–	168.62(13)
O4–Mo–O5	105.91(10)	106.29(10)	105.28(6)	106.93(14)
O4–Mo–O6	167.66(10)	170.09(8)	170.50(5)	–
O4–Mo–N2	94.38(10)	96.11(9)	89.17(6)	94.05(13)
O5–Mo–O6	86.24(9)	83.47(8)	83.49(5)	–
O5–Mo–N2	158.76(10)	156.71(9)	162.87(5)	156.49(14)
O6–Mo–N2	73.31(9)	74.00(7)	81.60(5)	–

i = −x+y,1−x,1/3+z

Table S5. $\pi\cdots\pi$ interactions (d(Cg3···Cg4)/Å) in **Ia**, **IIa** and **IIIa**.

complex	d(Cg3···Cg4) /Å	Cg3···Cg4(symmetry code)
Ia	3.733(3)	x,−1+y,z
IIa	3.7440(15)	x,−1+y,z
IIIa	3.7442(13)	1−x,−y,−z

Cg3 is the centroid of the ring N3, C3−C7 (in **Ia**, **IIa** and **IIIa**)
Cg4 is the centroid of the ring N4, C10−C12, C14−C15 (in **Ia**) and C10−C15 (in **IIa** and **IIIa**)

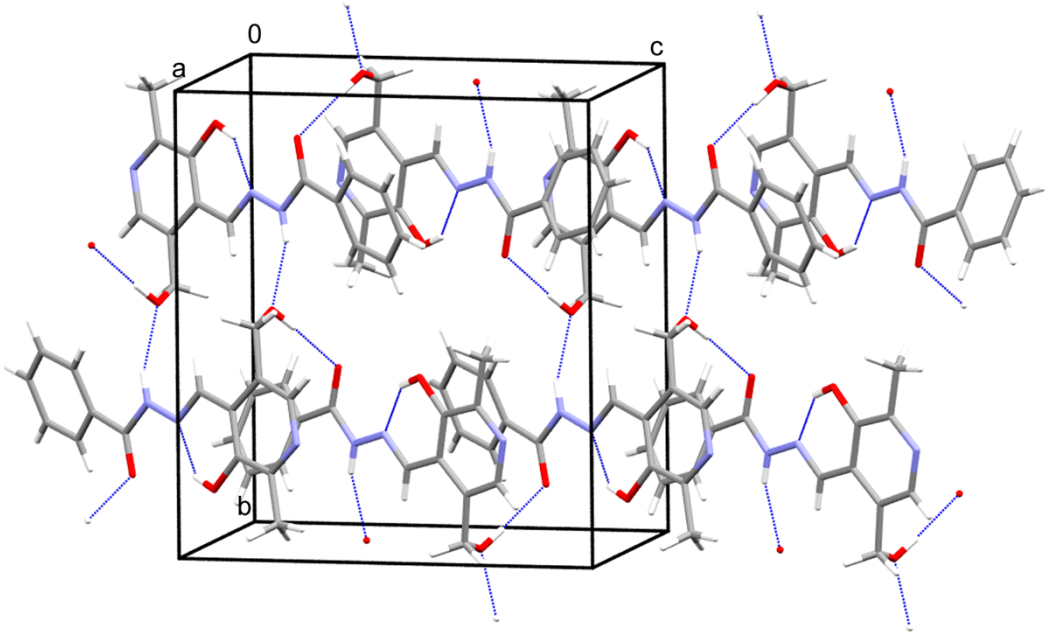

Fig. S6. The packing of $\mathbf{H_2L^2}$ molecules. Hydrogen bonds are presented by blue dotted lines.

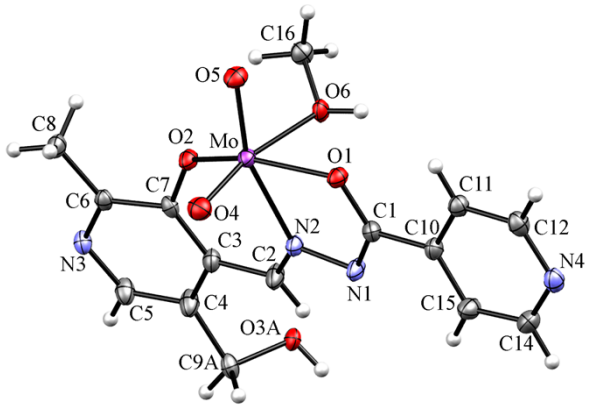

Fig. S7. Mercury – POV–Ray drawing of **Ia.** Thermal ellipsoids are at the 50% probability level. Only one position of the disordered pyridoxal is shown.

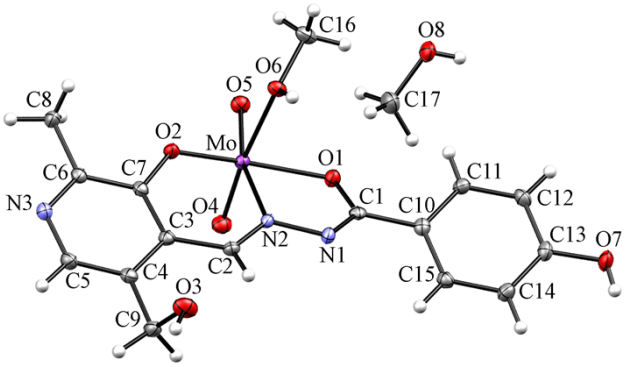

Fig. S8. Mercury – POV–Ray drawing of **IIIa.** Thermal ellipsoids are at the 50% probability level.

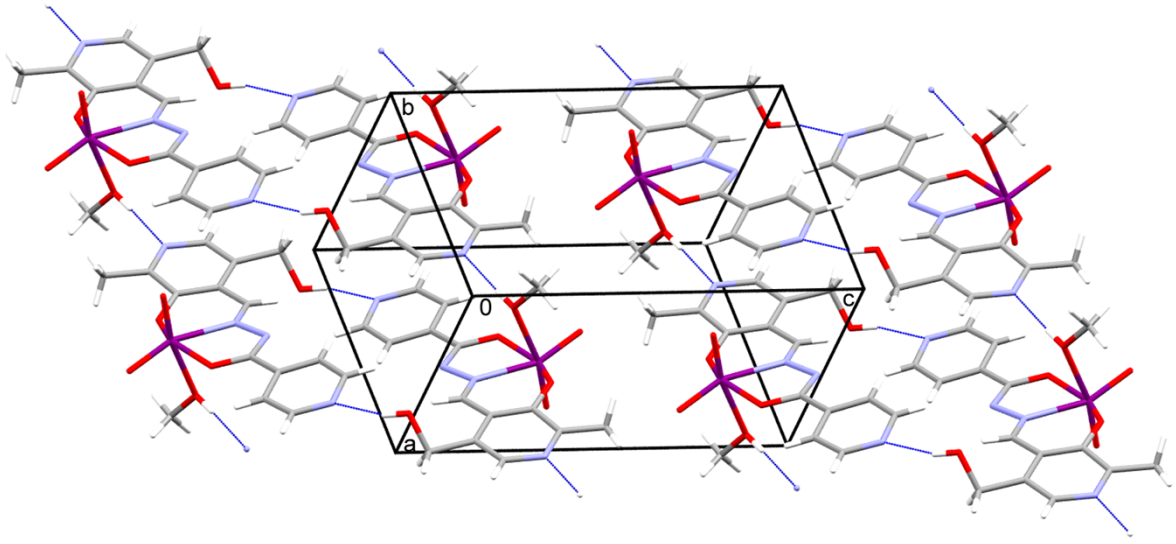

Fig. S9. The crystal packing of the **Ia.** Hydrogen bonds are presented by blue dotted lines.

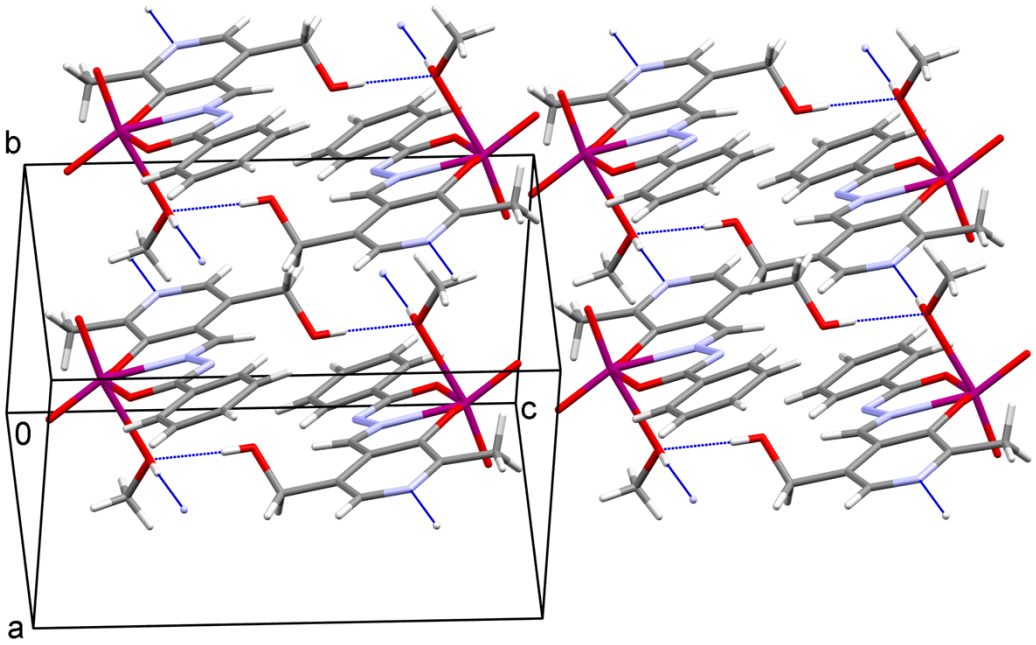

Fig. S10. The crystal packing of the **IIa**. Hydrogen bonds are presented by blue dotted lines.

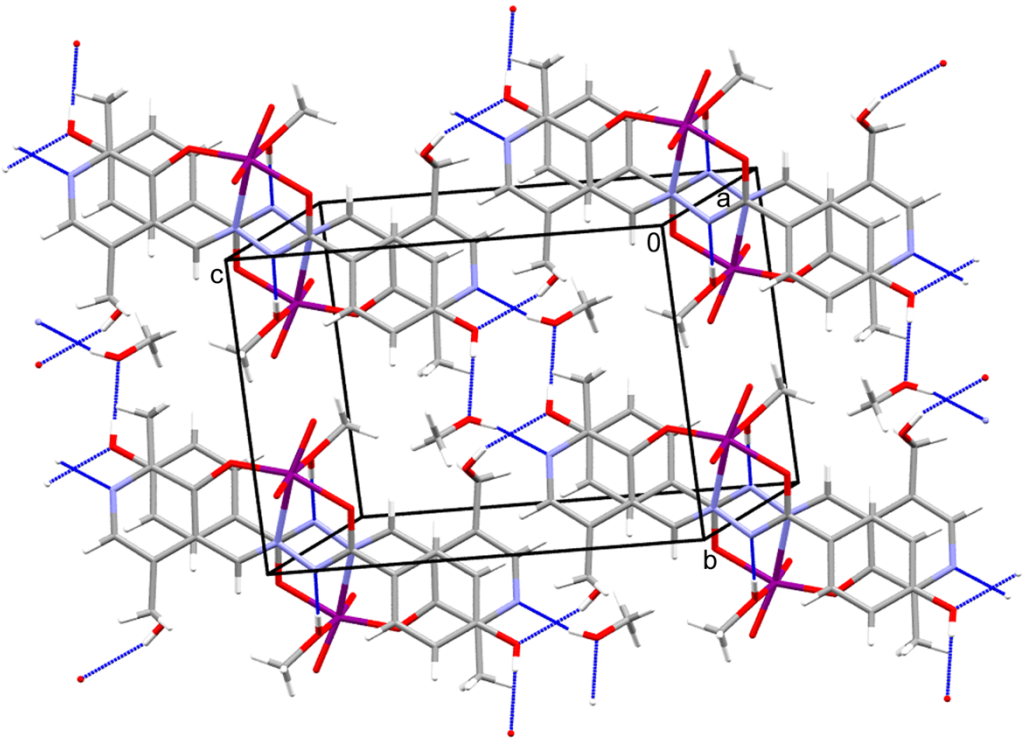

Fig. S11. The crystal packing of the **IIIa.** Hydrogen bonds are presented by blue dotted lines.

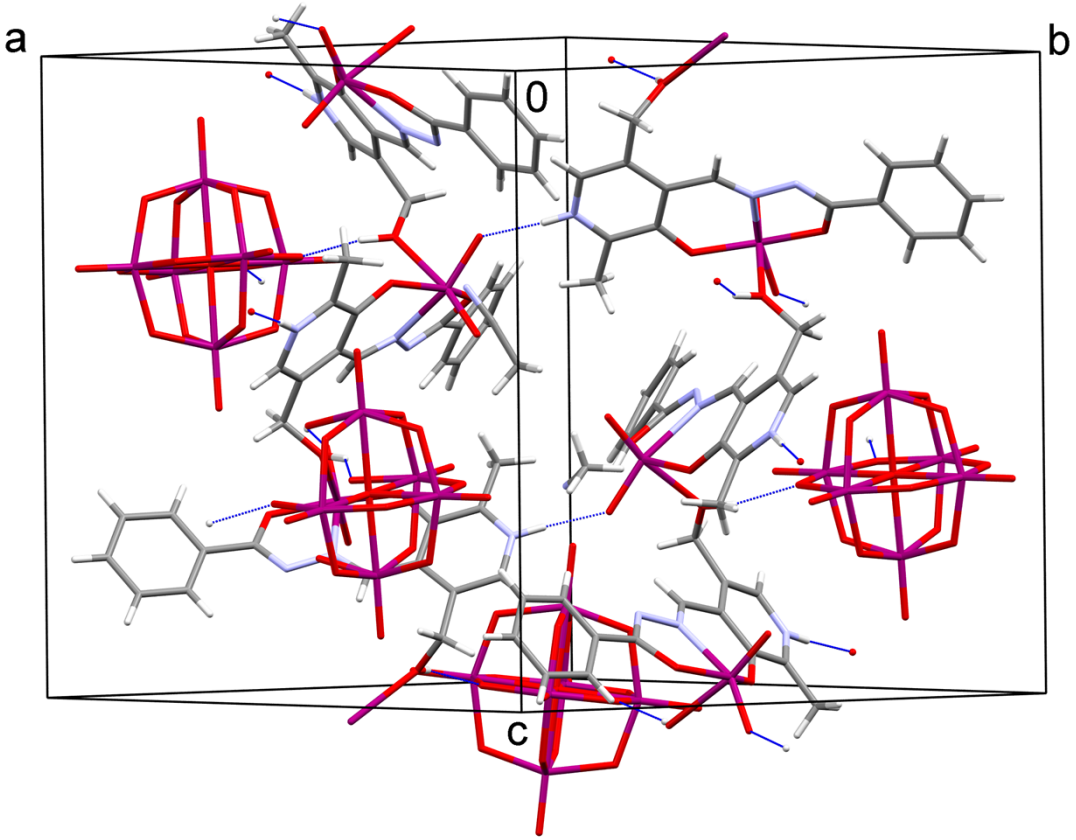

Fig. S12. The crystal packing of the **2.** Hydrogen bonds are presented by blue dotted lines.

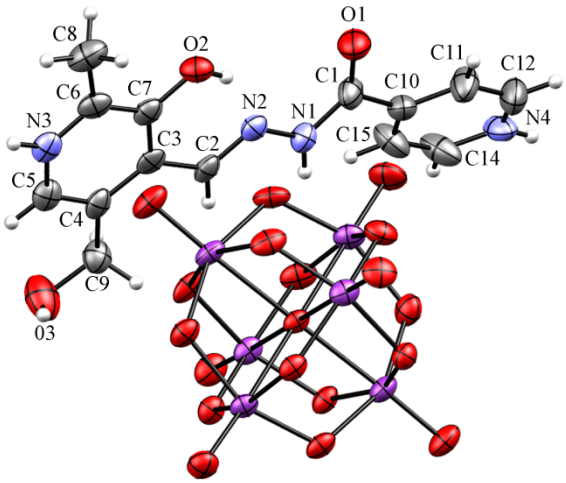

Fig. S13. Mercury – POV–Ray drawing of the complex **4.** Thermal ellipsoids are at the 50% probability level. Acetone molecules are omitted for clarity.

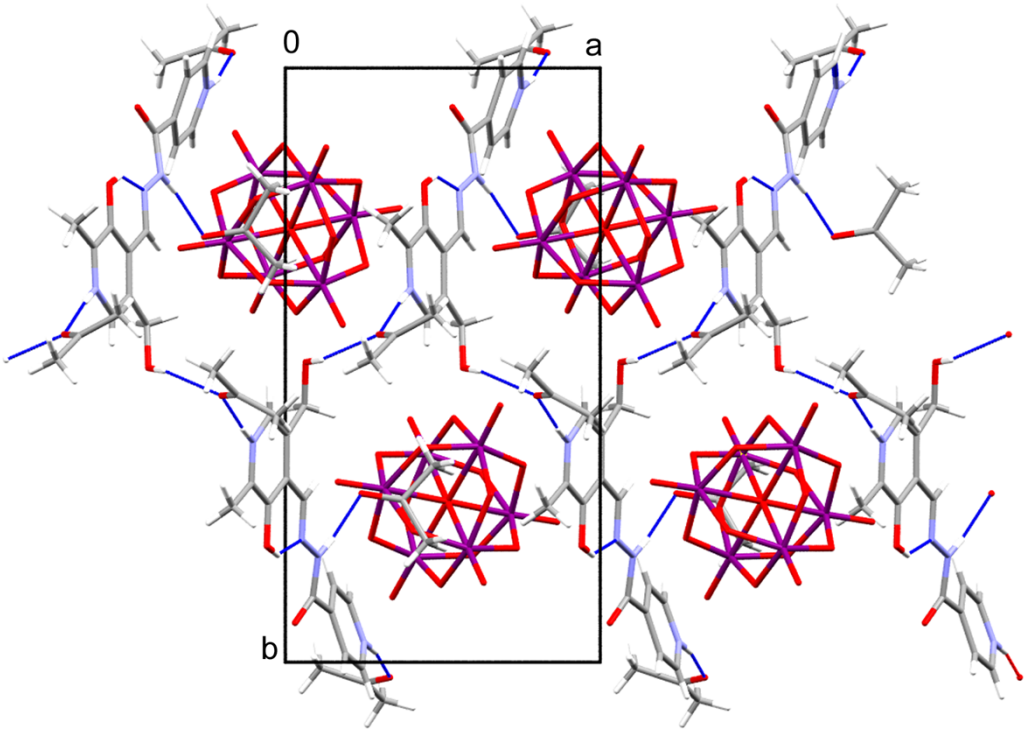

Fig. S14. The crystal packing of **4**. Hydrogen bonds are presented by blue dotted lines.

Catalytic studies

Scheme S2. Pyridoxal based *ONS* (on the left) and *ONS*·HCl ligands (on the right).

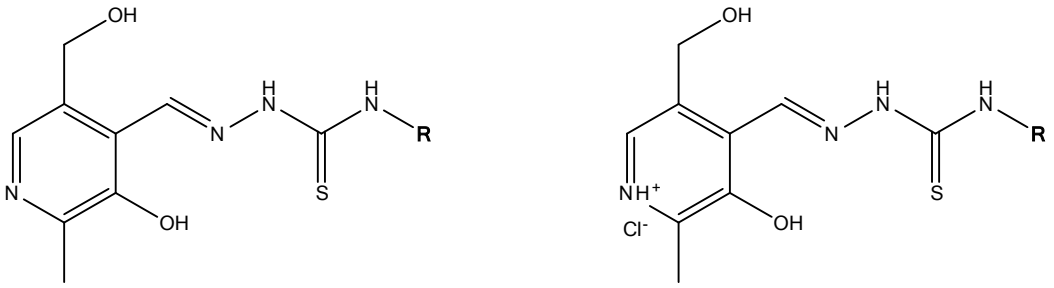

R_1 = H
R_2 = CH_3
R_3 = C_6H_5

Table S6. Relevant data of epoxidation catalyses with thiosemicarbazonato complexes:[1] neutral polynuclear **1**–**3** $[MoO_2L]_n$, charged polynuclear **1***–**3*** $\{[MoO_2(HL)]Cl\}_n$, neutral mononuclear **1a** $[MoO_2L(MeOH)]$ and charged mononuclear **1a*** $[MoO_2(L)(MeOH)]Cl$ complexes.

Complex	Conv. (%)[a]	Selec. (%)[b]	TOF_{20min} (h^{-1})[c]	TON[d]
1a*	48	74	480	960
1a	97	97	3360	1940
1*	70	82	787	1960
1	54	84	645	1040
2*	78	86	1080	1253
2	71	92	960	1420
3*	79	89	1680	1580
3	69	99	1080	1380

[a] for cyclooctene, calculated after 6 h. [b] formed epoxide per converted olefin after 6 h. [c] *n*(cyclooctene transformed) / *n*(catalyst) / time at 20 minutes. [d] *n*(cyclooctene transformed) / *n*(catalyst) at 6 h.

[1] (a) Pisk, J.; Agustin, D.; Vrdoljak, V.; Poli, R. *Adv. Synth. Catal*., **2011**, *353*, 2910–2914; (b) Pisk, J.; Prugovečki, B.; Matković-Čalogović, D.; Poli, R.; Agustin, D.; Vrdoljak, V. *Polyhedron*, **2012**, *33*, 441–449.